Journal Homepage: - www.journalijar.com
INTERNATIONAL JOURNAL OF ADVANCED RESEARCH (IJAR)
Article DOI: 10.21474/IJAR01/2871
DOI URL: http://dx.doi.org/10.21474/IJAR01/2871
ISSN NO. 2320-5407

RESEARCH ARTICLE

EFFECT OF IMPELLER TYPE AND ROTATIONAL SPEED ON FLOW BEHAVIOR IN FULLY BAFFLED MIXING TANK.

Adnan A. Abdul Rasool[1], Safaa S. Ahmad[1]. and F A Hamad[3]

1. Mech. Eng. Dept, College of Engineering, al-Mustansiriya University, Baghdad, Iraq.
2. Mech. Eng. Dept, College of Engineering, al-Mustansiriya University, Baghdad, Iraq.
3. School of Science & Engineering, Teesside University, Middlesbrough, TS1 3BA, UK.

Manuscript Info

Manuscript History

Received: 21 November 2016
Final Accepted: 21 December 2016
Published: January 2017

Key words:-
rotational speed, mixing, Pitched Blade, Chemineer.

Abstract

This paper reports the results of numerical study undertaken to investigate the effect of different impeller types and rotational speed on velocity field in mixing tank. The hydrodynamic of the flow in standard mixing tank generated by two impellers, Chemineer S-4 impeller (radial flow), Pitched Blade impeller (axial flow) is studied. ~~Using~~ ANSYS FLUENT v15.4. is used to solve the continuity and momentum equations incorporating the RNG K-ε turbulence model with the standard wall function available in Fluent. The multiple frames of reference (MFR) model is used for impeller modeling. The results show that the mixing performance of Chemineer impeller is better than the Pitched blade impeller at the same level of rotation speed.

Introduction

Mixing tank is one of the techniques that used and play a significant role in industrial processes to homogenize the mixture of two or more fluids/solids by using rotating impeller. The better understanding of the fluids behavior in mixing vessel may improve the performance of impeller and the mixing process. The main aims of using mixing are to improve the mass and heat transfer and to generate a homogenized mixture to minimize the settling of the particles at the bottom of the tank. A summary of some recent published works in the literature is given below.

Nienow, and Miles (1977) investigated the effect of impeller type and mixing tank configuration on fluid-particles mass transfer. **Ducoste and Clark** (1997) study the effect of tank size and impeller type on the turbulence in mixing tank. **Wei, et. al.** (1997) studied the influence of the number and width of baffles in mechanically mixing vessel with and without aeration on the fluid hydrodynamics and mixing tank. **Ducoste and Clark** (1999) employed the Computational Fluid Dynamics (CFD) in the study. The model was a simple geometry consists of the submerged impellers in cubical mixing vessel. The k-ε model was used to simulate the turbulence and the flow pattern induced in the vessel. **Masoud Rahimi** (2005) used CFD simulation to study the impellers number and layout on mixing time. A large storage tank of 19000m3 contain three types of crude oil with difference density.**Aoyi et. al.** (2008) investigated the hydrodynamics of fluid in mixing stirred vessel agitated by Rushton turbine with low clearance condition. The CFD technique and LDV measurements were performed in order to understand the flow pattern and mixing time.**Angelique Delafosse et. al.** (2008) investigated the hydrodynamics in mixing tank by CFD simulation. Two models were used to determine the dissipation rate and its distribution in mixing vessel. Three dimensional simulations using the commercial CFD code FLENT 6.2.16 based on the Unsteady Reynolds Averaged Naiver-Stokes equations (URANS) model and Large Eddy simulation (LES) model was used.

Corresponding Author:- Adnan A. Abdul Rasool.
Address: Mech. Eng. Dept, college of engineering, al-Mustansiriya University, Baghdad, Iraq.

In this paper, the flow field in stirred tank is studied using ANSYS Fluent (13) to identify the dead zones in the tank where the fluid is not mixing by presenting the velocity vectors at different planes in the tank. Two types of impellers (Pitched Blade and Chemineer S-4 Impellers) are used in this investigation to select the appropriate impeller for flocculation mixing process.

The CFD Model and Simulation

The CFD modeling of mixing problem, consist of three steps which are per-processing, equation solving and post-processing. In first part the problem geometry should be built and meshed. In the second step the partial differential equations describing the flow (Continuity and Navier-Stokes) are discretized on the mesh and solved simultaneously. The boundary and initial conditions should be introduced to the CFD. The turbulence model selected which is describing the effect of turbulence on the bulk flow properties of the fluid. Finally, the obtained results should be analyzed.

The CFD involves the numerical solution of conservation equations. In the present study, the simultaneous solution of continuity and Reynolds-averaged Navier –Stokes (RANS) equations together with the RNG of K-ε turbulent model were carried out using the finite control volume with cylindrical coordinates. The following equations were used in the model:

Continuity Equation:-

The net flow of mass across the boundary of a control volume is zero in steady state flow:

$$\nabla.\breve{G} = 0 \tag{1}$$

Where:

$\breve{G} = \rho\overline{V}$, is mass velocity.

Equation (1) can be written relative to cylindrical coordinates as follows:

$$\frac{\partial G_z}{\partial z} + \frac{1}{r}\frac{\partial}{\partial r}(rG_r) + \frac{1}{r}\frac{\partial G_\theta}{\partial \theta} = 0 \tag{2}$$

The subscripts z, r and ɵ are representing to the axial, radial and tangential components respectively. The $\overline{u}$, $\overline{v}$ and $\overline{w}$ are the components for the time mean velocity in z, r and ɵ directions respectively, and u′, v′ and w′ be the corresponding velocities of fluctuation. The continuity equation can be written as conservation of mass equation with the following form: (Joseph 1997), (Ronald 1984)

$$\frac{\partial}{\partial z}(\overline{u}) + \frac{1}{r}\frac{\partial}{\partial r}(r\overline{v}) + \frac{1}{r}\frac{\partial}{\partial \theta}(\overline{w}) = 0 \tag{3}$$

Momentum Equations:-

The general momentum equations in terms of shear stress τ governing the fluid motion for three dimensions for cylindrical coordinate are [9]:

In Z-direction

$$\rho\left(\frac{\partial U}{\partial t} + U\frac{\partial U}{\partial z} + V\frac{\partial U}{\partial r} + \frac{W}{r}\frac{\partial U}{\partial \theta}\right) = -\frac{\partial p}{\partial z} + \left[\frac{1}{r}\frac{\partial}{\partial r}(r\tau_{rz}) + \frac{1}{r}\frac{\partial}{\partial \theta}\tau_{\theta z} + \frac{\partial}{\partial z}\tau_{zz}\right] + \rho Fz \tag{4}$$

In R-direction

$$\rho\left(\frac{\partial V}{\partial t} + U\frac{\partial V}{\partial z} + V\frac{\partial V}{\partial r} + \frac{W}{r}\frac{\partial V}{\partial \theta} - \frac{W^2}{r}\right) = -\frac{\partial p}{\partial r} + \left[\frac{1}{r}\frac{\partial}{\partial r}(r\tau_{rr}) + \frac{1}{r}\frac{\partial}{\partial \theta}\tau_{\theta r} + \frac{\partial}{\partial z}\tau_{zr} - \frac{\tau_{\theta\theta}}{r}\right] + \rho Fr \tag{5}$$

In-θ-direction

$$\rho\left(\frac{\partial W}{\partial t} + V\frac{\partial W}{\partial r} + \frac{W}{r}\frac{\partial W}{\partial \theta} + \frac{WV}{r} + U\frac{\partial W}{\partial z}\right) = -\frac{1}{r}\frac{\partial p}{\partial \theta} + \left[\frac{1}{r^2}\frac{\partial}{\partial r}\left(r^2\tau_{r\theta}\right) + \frac{1}{r}\frac{\partial}{\partial \theta}\tau_{\theta\theta} + \frac{\partial}{\partial z}\tau_{z\theta} + \frac{\tau_{\theta r} - \tau_{r\theta}}{r}\right] + \rho F\theta \tag{6}$$

The previous equations of mass conservation and momentum can be combined to form of one general form (Versteeg 1995)

$$\frac{\partial \psi_z}{\partial z} + \frac{1}{r}\frac{\partial (r\psi_r)}{\partial r} + \frac{1}{r}\frac{\partial (r\psi_\theta)}{\partial \theta} = S_\Phi \quad (7)$$

For the continuity and momentum the ψz, ψr, and ψθ are the total diffusion fluxes defined by:

$$\psi_z = \rho U\phi - \Gamma_\phi \frac{\partial \phi}{\partial z} \quad (8)$$

$$\psi_r = \rho V\phi - \Gamma_\phi \frac{\partial \phi}{\partial r} \quad (9)$$

$$\psi_\theta = \rho W\phi - \Gamma_\phi \frac{\partial \phi}{r\partial \theta} \quad (10)$$

Where Φ stands for any of the dependent variables and the corresponding values of Γ_ϕ and S_ϕ is indicated in table (1).For axisymmetric swirling flow $\left(\frac{\partial \phi}{\partial \theta} = 0\right)$, equation (7) becomes:

$$\frac{\partial \psi_z}{\partial z} + \frac{1}{r}\frac{\partial (r\psi_r)}{\partial r} = S$$

$$\rho\frac{\partial}{\partial z}\left(U\phi - \Gamma_\phi \frac{\partial \phi}{\partial z}\right) + \frac{1}{r}\frac{\partial}{\partial r}\left(rV\phi - r\Gamma_\phi \frac{\partial \phi}{\partial r}\right) = S_\phi \quad (11)$$

Table 1:- variables of equations

Equation	Φ	ΓΦ	SΦ
Conservation of mass Eq(2)	1	0	0
Conservation of momentum in z – direction eq. (4)	U	μeff	$-\frac{\partial \bar{p}}{\partial z} + \frac{\partial}{\partial z}\left(\mu_{eff}\frac{\partial \bar{u}}{\partial z}\right) + \frac{1}{r}\frac{\partial}{\partial r}\left[r\mu_{eff}\left(\frac{\partial \bar{v}}{\partial z}\right)\right] + \frac{1}{r}\frac{\partial}{\partial \theta}\left[\mu_{eff}\left(\frac{\partial \bar{w}}{\partial z}\right)\right]$
Conservation of momentum in r – direction eq.(5)	V	μeff	$-\frac{\partial \bar{p}}{\partial r} + \frac{\partial}{\partial z}\left[\mu_{eff}\frac{\partial \bar{u}}{\partial r}\right] + \frac{1}{r}\frac{\partial}{\partial r}\left[r\mu_{eff}\frac{\partial \bar{v}}{\partial r}\right] + \frac{1}{r}\frac{\partial}{\partial \theta}\left[\mu_{eff}\left(r\frac{\partial\left(\frac{\bar{w}}{r}\right)}{\partial r}\right)\right] + \rho\frac{\bar{w}^2}{r} - \frac{2\mu_{eff}}{r}\left(\frac{1}{r}\frac{\partial \bar{w}}{\partial \theta} + \frac{\bar{v}}{r}\right)$
Conservation of momentum in Θ-direction eq.(6)	W	μeff	$-\frac{1}{r}\frac{\partial \bar{p}}{\partial \theta} + \frac{\partial}{\partial z}\left[\mu_{eff}\left(\frac{1}{r}\frac{\partial \bar{u}}{\partial \theta}\right)\right] + \frac{1}{r}\frac{\partial}{\partial r}\left[\mu_{eff}\left(\frac{\partial \bar{v}}{\partial \theta} - \bar{w}\right)\right] + \left[\frac{\mu_{eff}}{r}\left(r\frac{\partial\left(\frac{\bar{w}}{r}\right)}{\partial r} + \frac{1}{r}\frac{\partial \bar{v}}{\partial \theta}\right)\right] - \frac{\rho\bar{w}\bar{v}}{r} + \frac{1}{r}\frac{\partial}{\partial \theta}\left[\mu_{eff}\left(\frac{1}{r}\frac{\partial \bar{w}}{\partial \theta} + \frac{2\bar{v}}{r}\right)\right]$

The k-ε Turbulence Model:-

Jones and Launder had proposed the following equations for both the turbulence kinetic energy (k) and for energy dissipation (ε) [10], for turbulence kinetic energy (k)

$$\rho\bar{u}\frac{\partial k}{\partial z} + \rho\bar{v}\frac{\partial k}{\partial r} + \rho\bar{w}\frac{\partial k}{\partial \theta} = \frac{\partial}{\partial z}\left(\frac{\mu_t}{\sigma_{k,t}}\frac{\partial k}{\partial z}\right) + \frac{1}{r}\frac{\partial}{\partial r}\left(\frac{\mu_t}{\sigma_{k,t}}r\frac{\partial k}{\partial r}\right) + \frac{1}{r}\frac{\partial}{\partial \theta}\left(\frac{\mu_t}{\sigma_{k,t}}\frac{\partial k}{\partial \theta}\right) - \rho\varepsilon + \mu_t G \quad (12)$$

For energy dissipation rate (ε)

$$\rho\bar{u}\frac{\partial \varepsilon}{\partial z} + \rho\bar{v}\frac{\partial \varepsilon}{\partial r} + \rho\bar{w}\frac{\partial \varepsilon}{\partial \theta} = \frac{\partial}{\partial z}\left(\frac{\mu_t}{\sigma_{\varepsilon,t}}\frac{\partial \varepsilon}{\partial z}\right) + \frac{1}{r}\frac{\partial}{\partial r}\left(\frac{\mu_t}{\sigma_{\varepsilon,t}}r\frac{\partial \varepsilon}{\partial r}\right) + \frac{1}{r}\frac{\partial}{\partial r}\left(\frac{\mu_t}{\sigma_{\varepsilon,t}}\frac{\partial \varepsilon}{\partial \theta}\right) + C_1\frac{\varepsilon}{k}\mu_t G - C_2\frac{\varepsilon^2}{k} \quad (13)$$

Where G refers to the generation term and is given by [37]:

$$G = 2\left[\left(\frac{\partial \bar{u}}{\partial z}\right)^2 + \left(\frac{\partial \bar{v}}{\partial r}\right)^2 + \left(\frac{\bar{v}}{r}\right)^2\right] + \left[\left(\frac{\partial \bar{u}}{\partial r}\right) + \left(\frac{\partial \bar{v}}{\partial z}\right)\right]^2 + \left(\frac{\partial \bar{w}}{\partial z}\right)^2 + \left(\frac{\partial \bar{w}}{\partial r} - \frac{\bar{w}}{r}\right)^2 \quad (14)$$

The turbulent kinetic energy (k) and the dissipation rate of the turbulent energy (ε) are chosen as the two properties in order to determine the turbulent viscosity μ_t

$$\cdot \mu_t = \frac{C_\mu \rho k^{\frac{1}{2}}}{l^{-1}} \quad (15)$$

Where: Cμ is a constant. It is assumed that at a high Reynolds number, (ε) value to be Proportional to $k^{\frac{3}{2}} / l$, the above equation becomes:-

$$\mu_t = \frac{C_\mu \rho k^2}{\varepsilon} \quad (16)$$

The quantities σk,t , C1 , C2 , σε,t and Cμ that appear in the k-ε model and μt equations, are the universal k-ε model constants, whose values are reproduced in table (2) .

Table 2:- shows the variable of k-ε model.

Equation	Φ	ΓΦ	SΦ	C1	1.44
Turbulent K.E.eq. (12)	K	μt/σk,t	$-\rho\varepsilon + \mu_t G$	C2	1.92
Dissipation rate eq.(13)	ε	μt /σε,t	$\mu_t G C_1 \frac{\varepsilon}{k} - C_2 \frac{\varepsilon^2}{k}$	Cμ	0.09
				σk,t	1
				σε,t	1.3

Mixing time:-

Mixing time can be calculated from experimental relation referring to the concentration of tracer material which reach 99% using calculated tracer concentration in all tank fluid. (Harnby, 2001)

$$t = \frac{4.605}{(D_i/T)^b (D_i/T)^c} \quad (17)$$

Where a, b and c are constant depending on type pf impeller.

Model Stirred Tank Configuration:-

A schematic diagram of the tank and the impeller is shown in Fig. 1. The system consists of a flat bottomed cylindrical vessel, the diameter (Dt = 0.3 m) of which equals the height of the liquid (H=Dt). Four baffles having width, W=Dt/10 are spaced equally around the vessel. The shaft of the impeller is concentric with the axis of the vessel. The Impeller diameter, Di, equivalent to Dt /3. The distance between the tank bottom and the impeller position C is set to C= Dt /3. The rotational speed of the impeller, N, is ranging from 60 rpm to 135 rpm increasing step 15 rpm, leading to a tip speed, Vtip, ranging 0.314 m/s to 1.05 m/s. The working fluid is water with density, ρ, of 1000 kg/m3 and viscosity, μ, of 1×10-3 Pa.s. The mixing tank as showed Fig.1 was design in depends on the standard configuration as follow: [1], (Georgy 1991). The two types of impellers: Chemineer S-4 and pitched blade impeller as shown in Fig.2, the specification of the impellers are show in table (3).

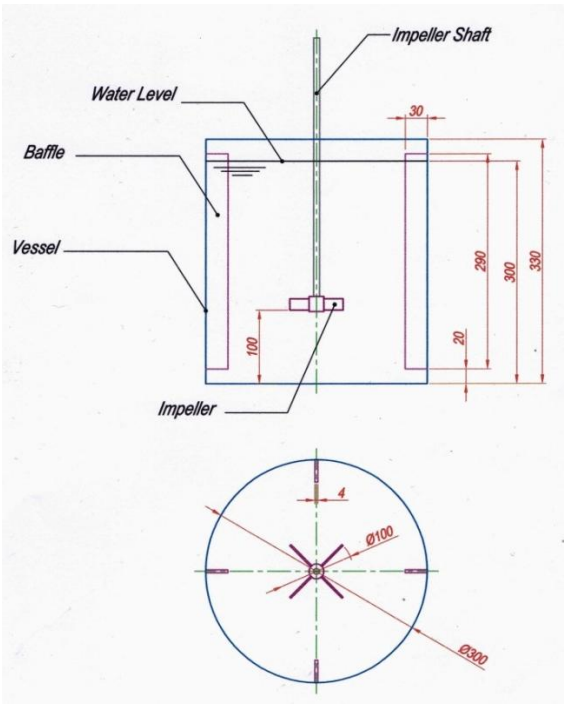

Fig. 1:- mixing Tank in Present Study

Table 3:- Specification of Impeller.

Specification	Impeller type	
	Chemineer S-4	Pitched Blade
No. of blades	4	4
Blade width at tip (m)	0.016	0.02
Blade width at root (m)	0.016	0.02
Blade thickness	0.003	0.003
Hub cord angle (deg.)	90	45
Hub Diameter (m)	0.2	0.2
Hub height (m)	0.2	0.2

The Numerical Solution Setup

In the present study, mixing in 21.2 liter of water agitated by three types of impellers. The impellers rotation speeds were ranging from 60 to 135 rpm. The mixing tank model was divided in to 58244 nodes as shown in Fig.3. The MFR method was applied for modeling the impeller rotation. Also the continuity and Navier-Stokes equations together with the RNG version of the K-Ɛ were used to describe the equation of motion (13).

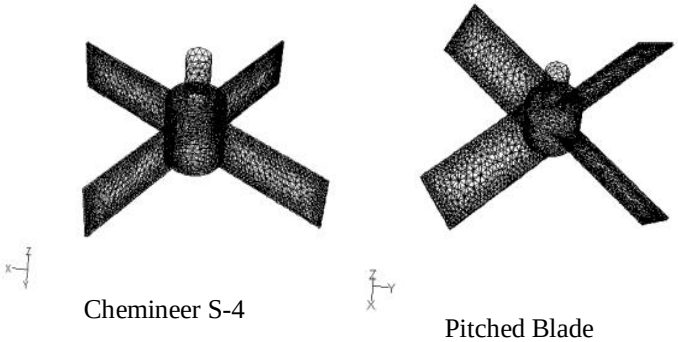

Chemineer S-4 Pitched Blade

Fig 2:- Impeller Modeling and Mesh Geometry.

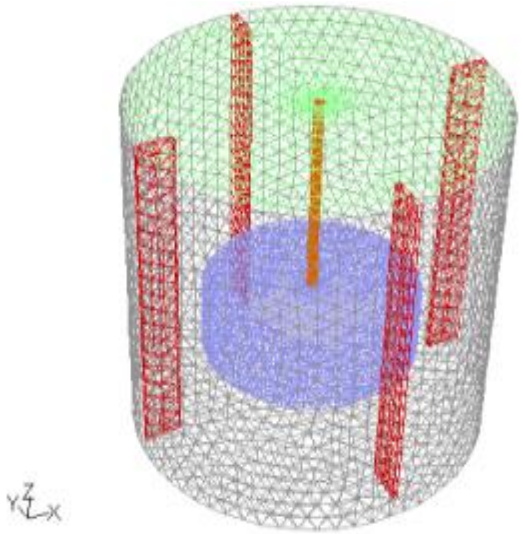

Fig 3:- The Mixing Tank Modeling and Mesh Geometry.

Results and Discussions

The impellers rotation speed has a great effect on fluid motion in mixing processes. Consequently, the efficiency of settling process for the solid material is affected by the changing of impeller rotation speed. Also, the concentration of chemical additives would become more homogeneous when the optimum impeller rotation speed has been correctly selected.

Fig.4 and Fig.5 illustrated the velocity vectors, contour and graph for Z-θ and Z-R planes for Pitched Blade impeller rotated at 60 rpm. At the Z-θ plane 0 degree, the impeller pumping the fluid toward the bottom of the tank, and then moved with high velocity toward the upper zone near the baffle surface because the baffles help the circulated fluid to flow upward to the upper zone of the tank instead of circulation. This fluid motion produced a circular mixing zone (eddy) at which the fluid circulated around the specific point located at 0.11m from the center of tank with height of 0.54m from the base surface which is almost half the clearance between the impeller and the bottom of tank.

The average velocity of fluid is in varied with the radius of the tank. Thus, two poor mixing zones are generated at center of the bottom of the vessel also at the free surface of fluid. The same behavior of fluid is repeated in Sec.30º, and Sec60º but the average velocity of fluid decreases when the fluid motion toward the upper zone of the vessel due there are no baffles existed at those sections. At Sec. 90 degree it is easy to note that the fluid motion is identical with the fluid flow at Sec.0 degree.

In Z-R plane as shown in Fig. 5 at height 0.01m from the bottom of the tank the fluid flow generates a low velocity zone at the center of plane , this zone about 0.085m in diameter. At height 0.1m the fluid velocity is highly fluctuated due to the high influence of impeller pumping capacity as well as the effect of circulation fluid which decrease the velocity of pumped fluid which produces the eddy as explained earlier. The low velocity mixing zone is located between the impeller zone and the tank wall having an annulus shape of inner diameter about 0.038m and 0.24m in outer diameter. The fluid velocity is increased near the baffles with impeller rotation direction is clockwise, resulting in part of the fluid flow toward the upper zone of tank and the rest return to impeller zone with high velocity. The fluid flow changes from highly fluctuated to more moderate motion at height of 0.2m which reflects the effect of rotational motion of impeller. The effect of baffles is quite clear by producing poor mixing zones located between them. The velocity increases as height increased until reached 0.3m height at which the eddies length scale become small and circulated toward the shaft of impeller due to the effect of pumping from impeller.

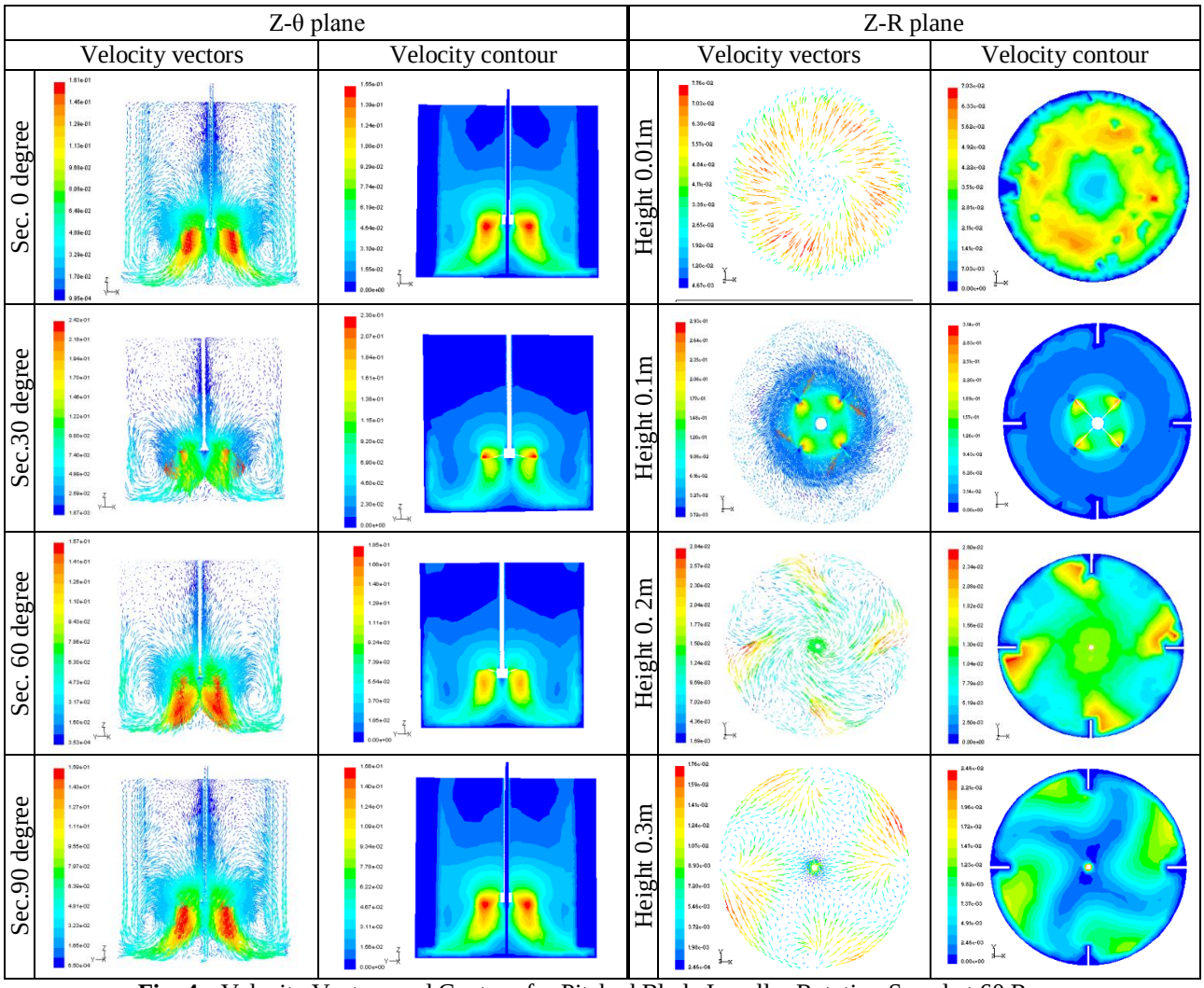

Fig. 4:- Velocity Vectors and Contour for Pitched Blade Impeller Rotation Speed at 60 Rpm.

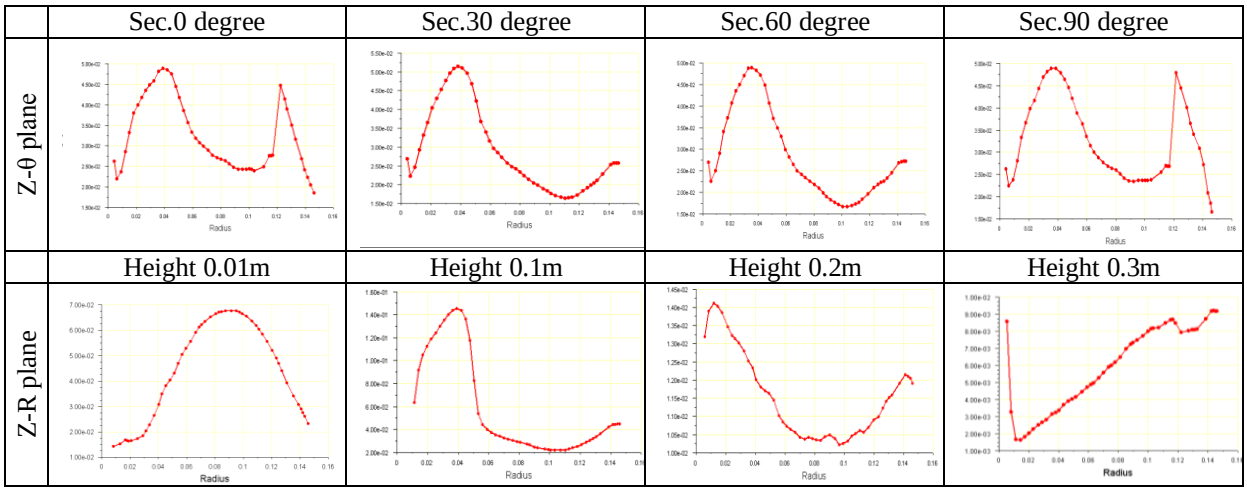

Fig. 5:- Velocity graph for Pitched Blade Impeller Rotation Speed at 60 Rpm in Z-θ and Z-R planes.

Fig.6 shows the velocity vectors and contours for Chemineer S-4 impeller rotates at 60 rpm. The velocity vectors for 0º plan show that the impeller blades pumped the fluid radially to ward tank wall that cause fluid to split into two

jets. The small jet is circulated downward to the bottom of tank and then returns to the impeller zone so produces an eddy in the zone below the impeller. The center of eddy is located at radius of 0.103 m from the tank center and 0.064m from the bottom of tank. A Poor or weak mixing region is existed at the center of tank below the impeller.

The second jet of the fluid will be circulated in upward direction, so generate an eddy which is located at same radial direction with lower one but with height of 0.134m from the bottom of tank. The flow pattern will be same at 30º and 60ºplans except the reduction in the fluid flow velocity at the upper zone especially at 30º plan and velocity of fluid near the wall of tank increases in the upward direction. The fluid flow behavior in 90º plan is similar to that observed at 0º plan.

In Z-θ direction at height 0.01 m velocity vectors and contour shows the poor mixing zone in the center of tank. The velocity increases toward the wall of tank, then the velocity decreases near the tank wall, this fluctuation of velocity lead to form annular ring zone with high mixing. At height of 0.1m (impeller zone) the velocity linearly increases along the blade of impeller until it reaches to its maximum value at the tip of the blade. Then the velocity is sharply decreases because of fluid circulation as a result of the direction of pumping direction.

At height 0.2 m most of fluid is split into four symmetrical jets and the other flows upward direction reaching the free surface. These symmetrical jets are radially circulated in the mixing plan thus, eddies were generated as the flow become close to the wall of the baffles. The fluid flow far from the wall of baffles still circulate with high velocity in the radial direction toward the center of tank that lead to generate a high mixing zone. At the free surface of fluid the velocity decreases because most of the fluid circulates in the lower zone due to the influences of impeller pumping capacity. The high mixing zone reduces especially at the center of tank but swirling motion continues near the baffles wall.

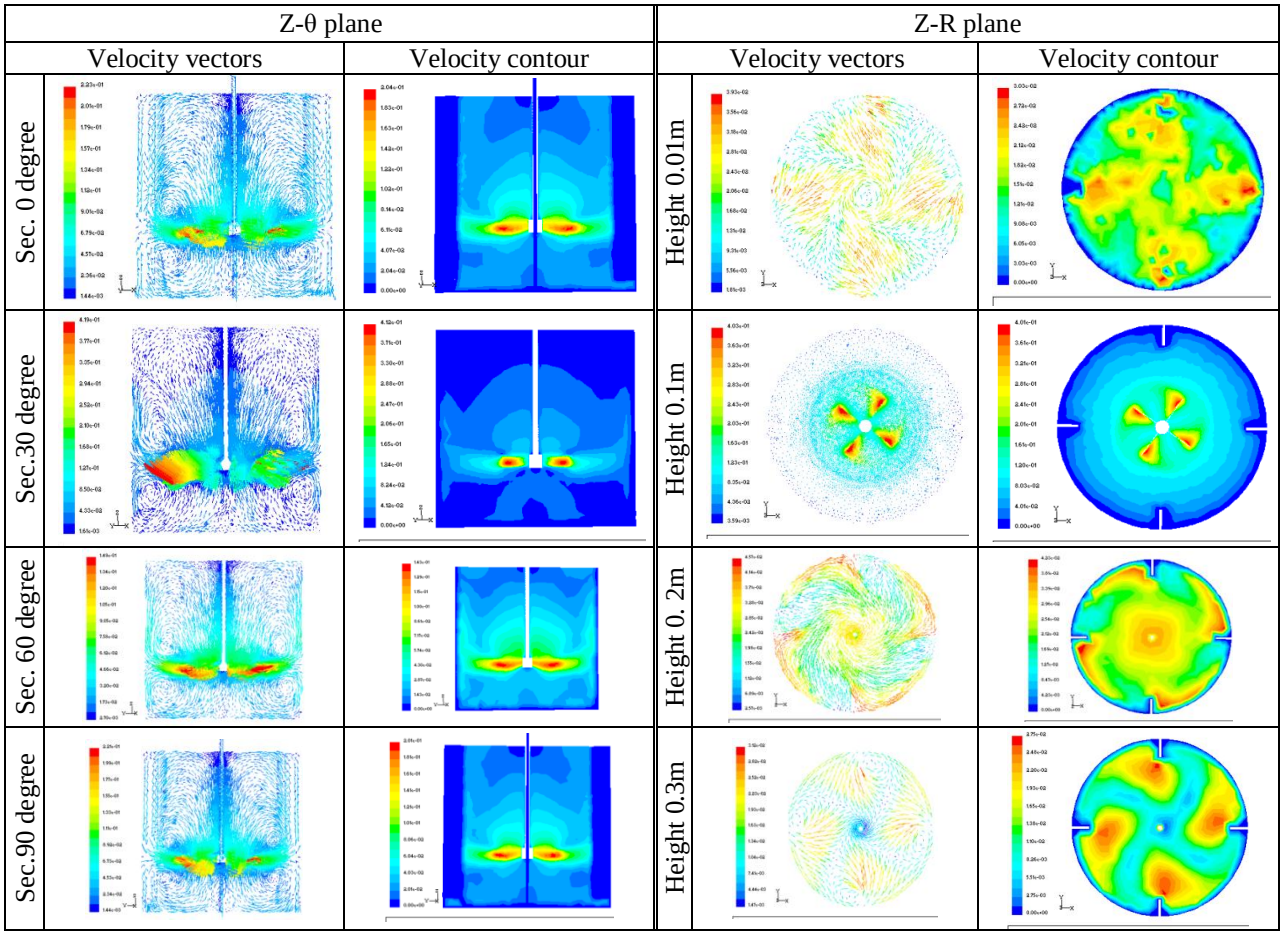

Fig. 6:- Velocity Vectors and Contour for Chemineer S-4 Impeller Rotation Speed at 60 Rpm

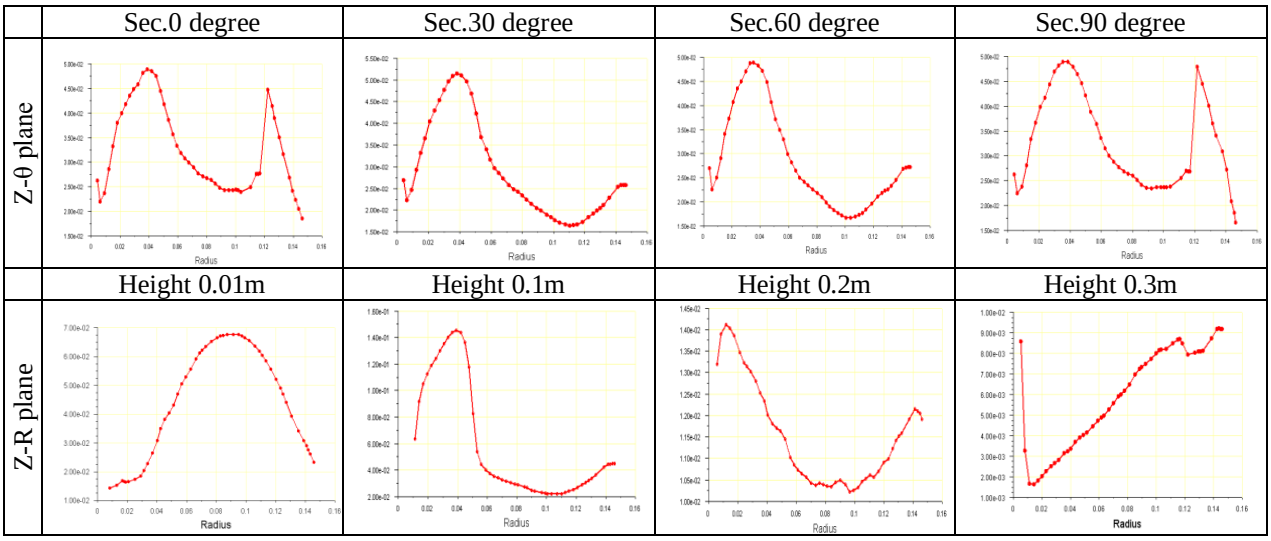

Fig. 7:- Velocity graph for Chemineer S-4 Impeller Rotation Speed at 60 Rpm in Z-θ and Z-R planes

Fig.8 shows the difference between the flow patterns induced by Pitched blade and Chemineer impellers with both rotates at 90 rpm. The difference can be observed in both Z-θ and Z-R planes. The Pitched blade impeller influence the all tank while Chemineer impeller influence the mixing in 2/3 of the tank at same rotation speed. The velocity of fluid flow in mixing tank agitated by Chemineer impeller is higher than that induced by pitched blade impeller as showed in Fig.9 Thus the mixing time with Chemineer impeller is less than that with Pitched blade one.

Fig.10 illustrated the velocity of the fluid in the mixing tank in Z-R plane with height 0.1 m from the bottom of the tank. The Chemineer impeller produces a fluid flow with a high velocity as well as the high velocity fluctuated in comparison with the Pitched Blade impeller. In the height of 0.1 , 0.2 and the free surface of the fluid, it easy to note that the similarity with velocity fluctuated produced by both impellers but still Chemineer impeller produce fluid motion higher than that produces by Pitched Blade impeller as shows in Fig. 11,12 and 13. In the Z-θ plane the velocity of fluid generated by both impellers is similar in the fluctuation and closer in values for all sections as shows in Fig. 14 and 15.

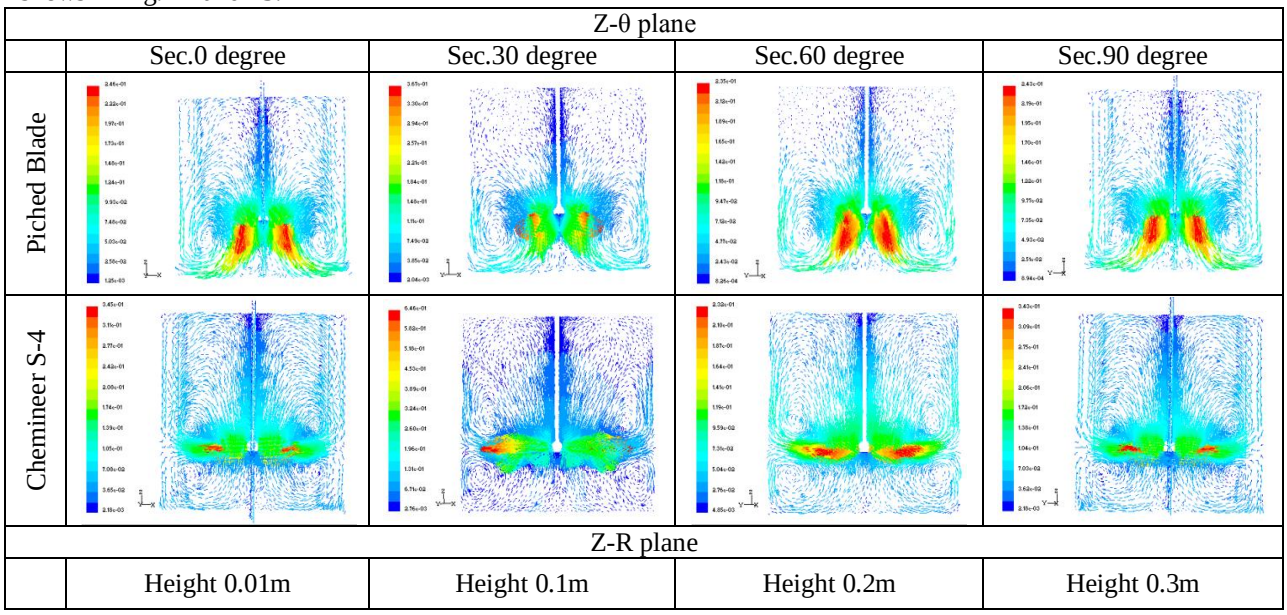

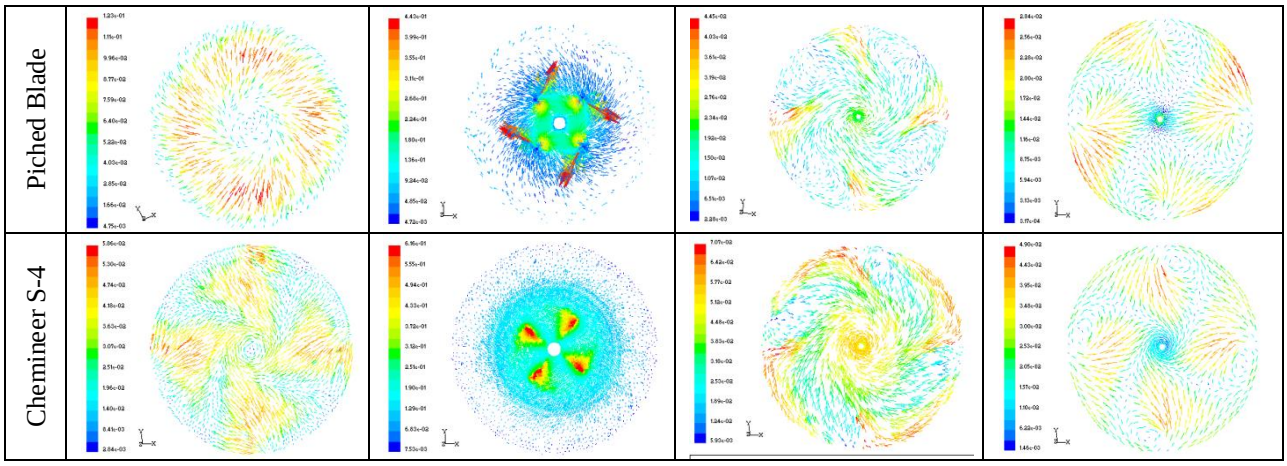

Fig. 8:- Velocity Vectors for Pitched Blade and Chemineer S-4 Impellers Rotation Speed at 90 Rpm

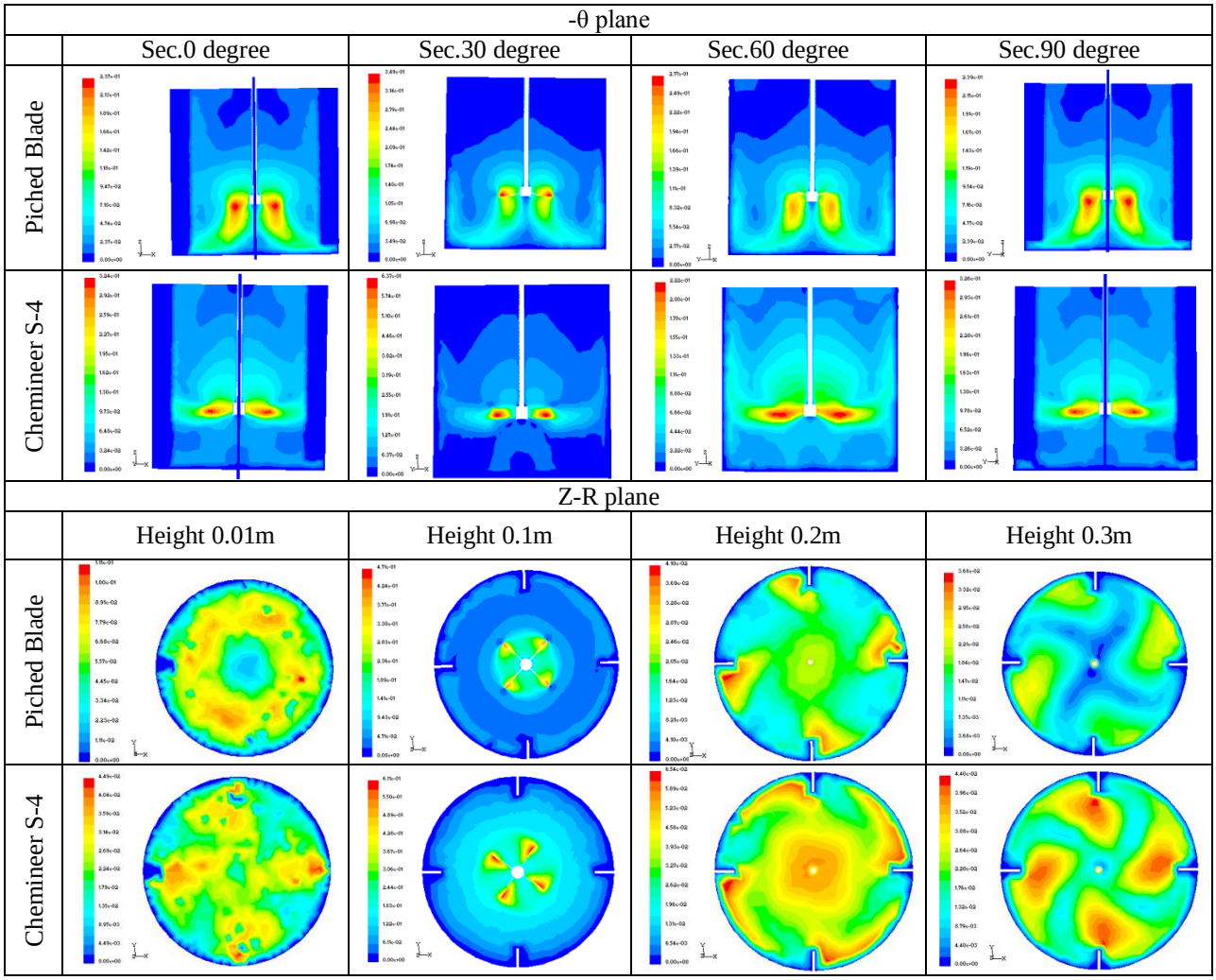

Fig. 9:- Velocity Vectors and Contour for Pitched Blade Chemineer S-4 Impeller Rotation Speed at 90 Rpm

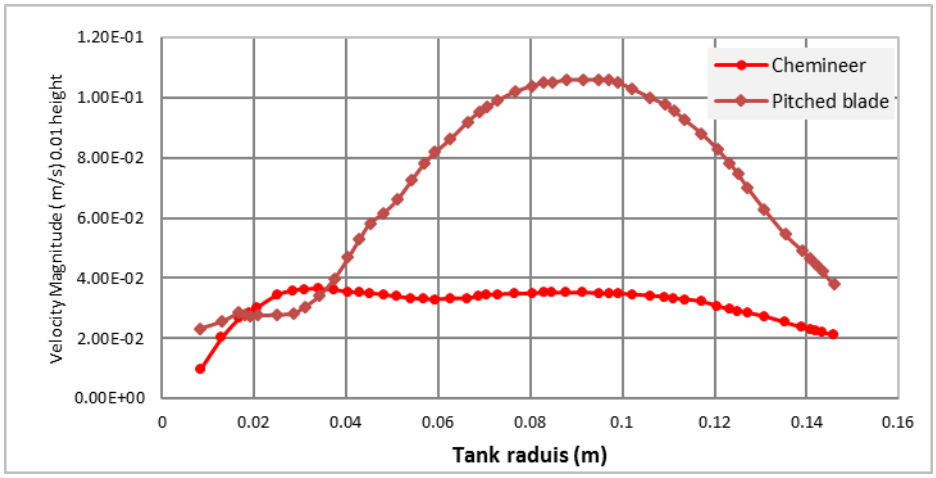

Fig. 10:- Velocity graphs for Pitched Blade and Chemineer S-4 Impeller Rotation Speed at 90 Rpm at Z-θ plane Height 0.01m

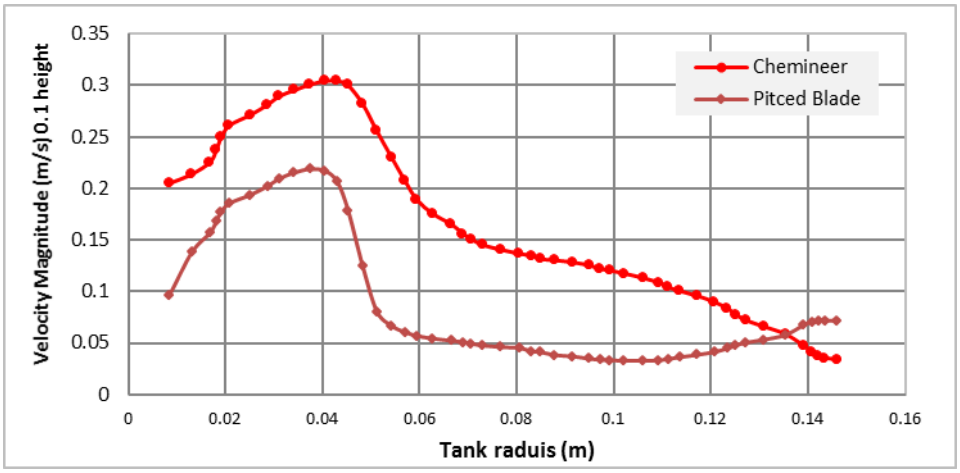

Fig. 11:- Velocity graphs for Pitched Blade and Chemineer S-4 Impeller Rotation Speed at 90 Rpm at Z-R plane Height 0.1 m

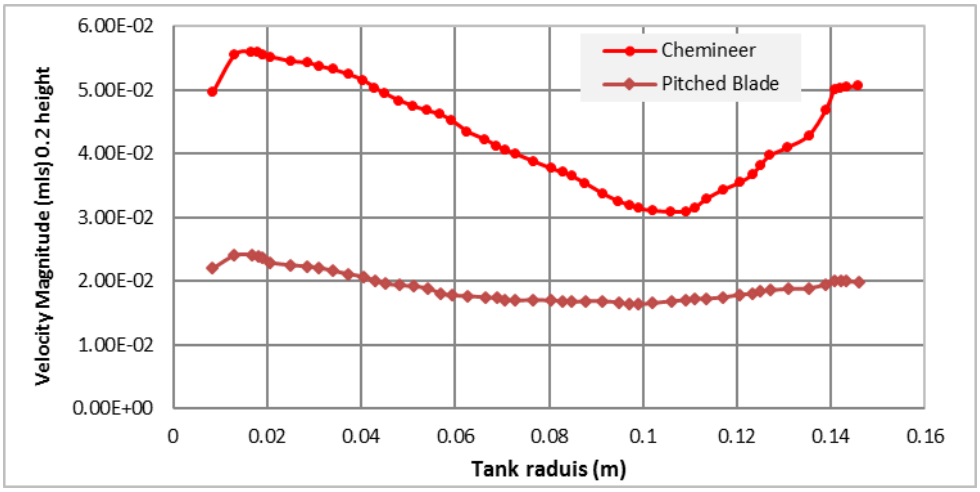

Fig. 12:- Velocity graphs for Pitched Blade and Chemineer S-4 Impeller Rotation Speed at 90 Rpm at Z-R plane Height 0.2 m

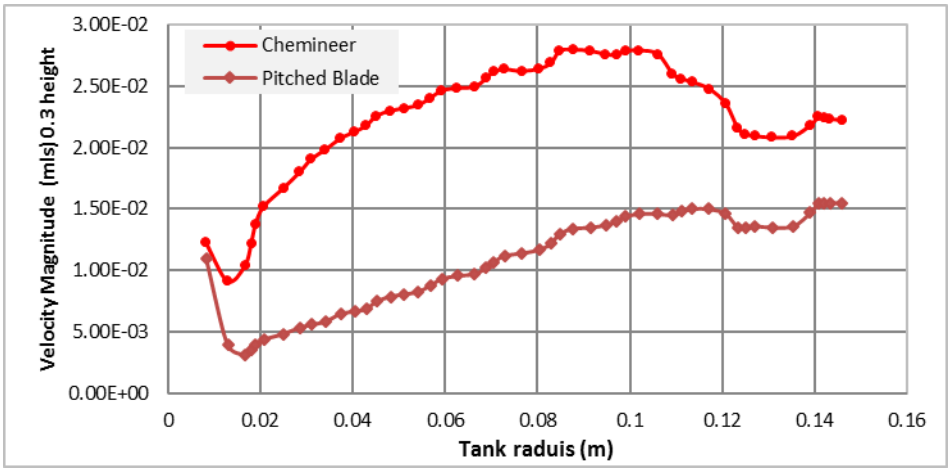

Fig. 13:- Velocity graphs for Pitched Blade and Chemineer S-4 Impeller Rotation Speed at 90 Rpm at Z-R plane Height 0.3 m

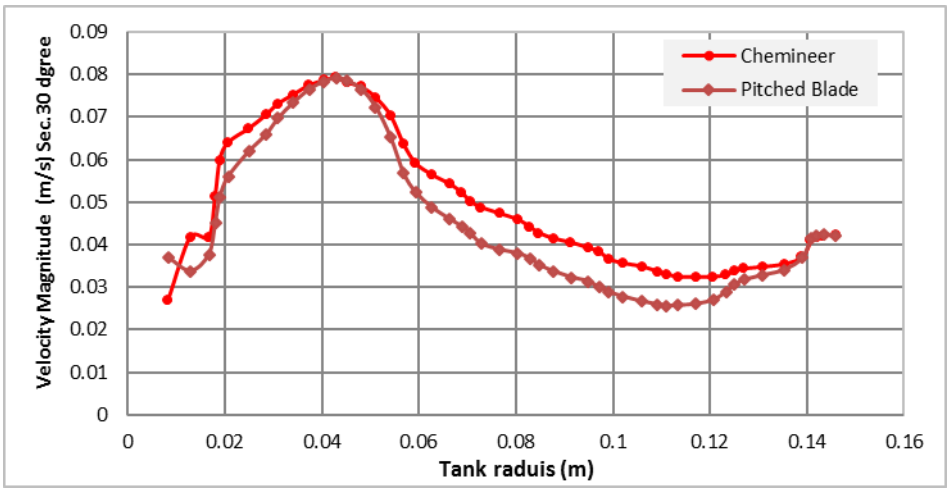

Fig. 14:- Velocity graphs for Pitched Blade and Chemineer S-4 Impeller Rotation Speed at 90 Rpm at Z-R plane Sec. 30 degree.

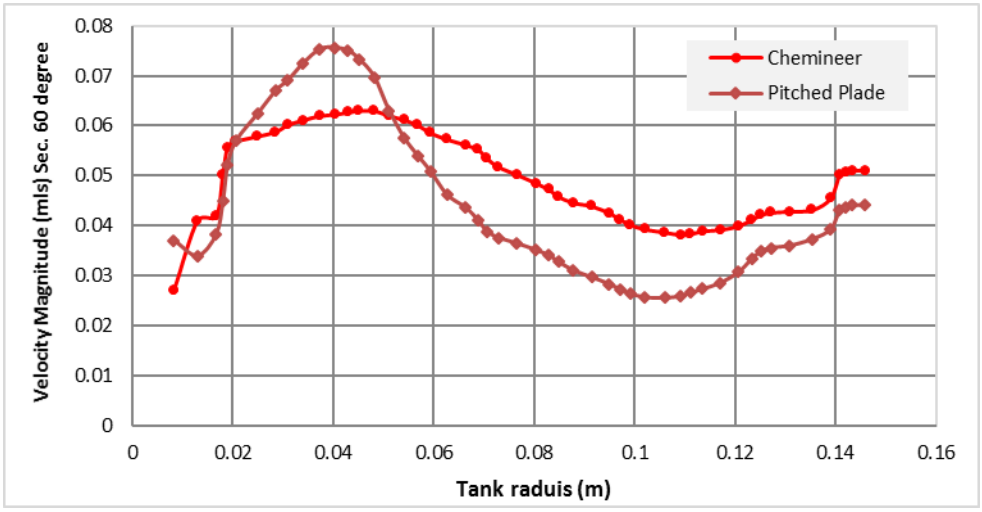

Fig. 15:- Velocity graphs for Pitched Blade and Chemineer S-4 Impeller Rotation Speed at 90 Rpm at Z-θ plane Sec. 60 degree.

The mixing time depend on both the fluid flow pattern and fluid velocity, hence the Chemineer impeller produce fluid flow with high velocity and shorter paths than that generates with Pitched Blade impeller thus the mixing equipped with Chemineer impeller is less in time than with Pitched Blade impeller as Shows in Fig. 16.

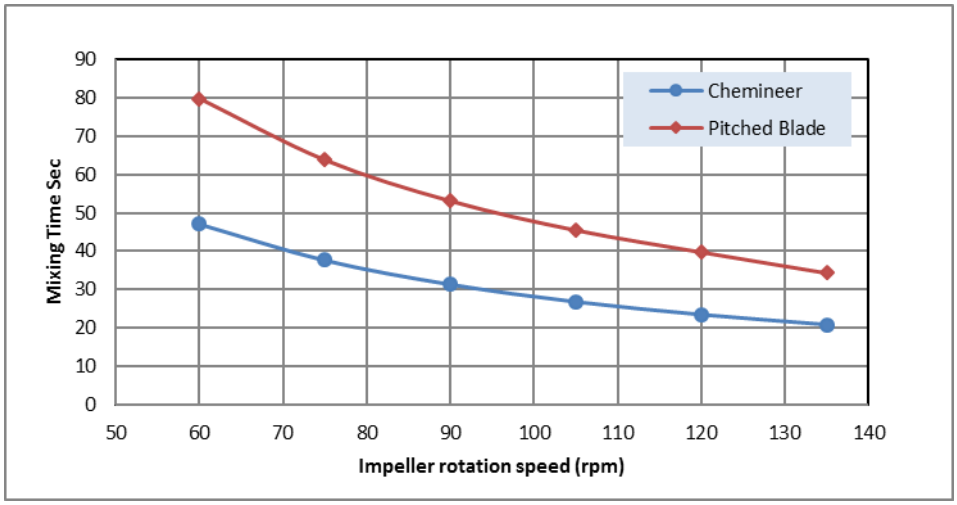

Fig 16:- Mixing Time for Pitched Blade and Chemineer S-4 Impellers.

Nomenclature:-

Symbols	Description	SI Unit
a	Acceleration	m/s2
C0	Constant	
C1	Constant	
C2	Constant	
Cμ	Constant	
D_i	Impeller diameter	m
D_t	Diameter of mixing tank	m
E_k	Turbulent kinetic energy in equation	m2/s2
C	Impeller clearance	m
H	Liquid height in mixing tank	m
N	Impeller rotation speed	rev/min
p	Pressure	N / m2
r	Radius of mixing tank	m
Sr	Source term in r-direction of momentum equation	
S_θ	Source term in θ-direction of momentum equation	
S_k	Source term in k-ε model	
S_ε	Source term in k-ε model	
t	Mixing time	s
U	Velocity vector in z - direction	m / s
u	Velocity in z-direction	m / s
V	Velocity vector in θ - direction	m / s
v	Velocity in r-direction	m / s
W	Velocity vector	m / s
w	Velocity in θ – direction	m / s
ρ	Density	kg / m3
ε	Dissipation rate of kinetic turbulence energy	m2 / s3
ε_w	Dissipation rate of kinetic turbulence energy at wall	m2 / s3
ε_e	Eddy viscosity	Pa.s
Γ	Arbitrary parameter	

Conclusions

The FLUENT v.15.4 is used to analysis the Pitched Blade and Chemineer impeller used for mixing purpose in cylindrical mixing tank. The following conclusions and the results of the study:

1. The numerical analysis gives good results of velocity distribution and mixing rate with the tank. Such results can be used for describing the flow behavior and the difference between the two used impellers
2. Velocity vectors show that the poor mixing zone is generated with Pitched Blade impeller is less than that generated with Chemineer impeller.
3. The fluid flow velocity generated with Chemineer impeller is higher than that generated with Pitched Blade.
4. The fluid flow velocity is similar in the distribution behavior for Z-θ and Z-R planes but noted a difference in the magnitude for the two impellers.

References

1. W. Nienow, D. Miles "The Effect of Impeller / Tank Configuration on Fluid-Particle Mass Transfer" Elsevier Sequoia, The Chemical Engineering Journal, vol.15, pp.13-24, 1978.
2. Joel J. Ducoste, Mark M. Clark, " Turbulence in Flocculators: Effect of Tank Size and Impeller Type", AIChE. Journal, vol.43, No. 2, pp.328-338, February, 1997.
3. Wei-Ming Lu, Hong-Zhang Wu and Ming-Ying Ju, " Effect of Baffle design on the Liquid Mixing in an Aerated Stirred Tank with Standard Rushton Turbine Impeller", Pergamon, Chemical Engineering Science , vol.52, No.21:22, pp.843-3851, 1997.
4. Joel J. Ducoste, Mark M. Clark, "Turbulence in Flocculators: Comparison of Measurements and CFD Simulations" AIChE. Journal, vol.45, No.45, pp.432-436, February, 1999.
5. Masoud Rahimi, "The Effect of Impellers Layout on Mixing in a Large-Scale Crude Oil Storage Tank" Elsevier, Journal of Petroleum Science & Engineering, vol. 46, pp.161-170, 2005.
6. Aoyi Ochieng, Maurice S. Onyango, Anil Kumar, Kirimi Kiriamiti, Paul Musonge "Mixing in a Tank Stirred by a Rushton turbine at Low Clearance", Elsevier, Chemical Engineering and Processing, vol.47, pp.842-851, 2008.
7. Angelique Delafosse, Alain Line, Jerome Morchain and Pascal Guiraud, "LES and URANS Simulation of Hydrodynamics in Mixing Tank: Comparison to PIV Experiments", [8] Elsevier, Chemical engineering Research and Design, vol.86, pp.1322-1330, 2008.
8. Joseph H. Spurk “Fluid Mechanics “. Translated by Kathrine mayes , Springer-Verlag Berlin Germany , 1997. PP: 147.
9. Ronald l. panton “Incompressible Flow “. A Wiley–interscience publication, John Wily and Sons, 2nd edit. , 1984.
10. Versteeg, H.K. and W. Malasekera, "An Introduction to Computational Fluid Dynamics, the Finite Volume Method”. Longman scientific and technology, 1995.
11. Georgy T., Franklin, L. Burton “Wastewater Engineering, Treatment, Disposal, and Result “. McGraw-Hill series in water resources and environmental engineering, 3rd edi. , 1991. PP: 217.
12. N. Harnby, M. F. Edwards, A. W. Nienow "Mixing in the process industries" Butterworth – Heinemann, second edition, 2001.
13. Ansys Fluent 13: theory guide. U.S.A.: Ansys Inc.; 2011